INTERNATIONAL JOURNAL OF TECHNICAL RESEARCH STUDIES (IJTRS)
(Open Access, Double-Blind Peer Reviewed Journal)
ISSN Online: ISSN Print

GIS-Based Land-Use Planning For Sustainable Urban Growth

PK Anilkumar

Interior Designer, Thrissur, India

Article information

Received: 17th December 2025
Received in revised form: 21st January 2026
Accepted: 12th February 2026
Available online: 9th March 2026

Volume: 2
Issue: 1
DOI: https://doi.org/10.5281/zenodo.20132853

Abstract

Uncontrolled urban expansion threatens agricultural productivity, biodiversity corridors, and flood resilience across rapidly growing cities in Sub-Saharan Africa. This study applies Geographic Information System (GIS) based multi-criteria decision analysis (MCDA) and Cellular Automata–Markov (CA-Markov) modelling to evaluate land-use change and guide future development in the Kumasi Metropolitan Area, Ghana. Landsat imagery from 2000, 2010, and 2020 was classified into five land-cover categories using supervised Maximum Likelihood classification (overall accuracy > 87%, Kappa > 0.82). Between 2000 and 2020, built-up area expanded from 42.3 km² to 95.6 km², consuming 38.5 km² of vegetation and 20.2 km² of agricultural land. An Analytic Hierarchy Process (AHP) weighted overlay identified zones with high development suitability based on slope, road proximity, soil type, and flood risk. CA-Markov simulations projected three 2030 scenarios: business-as-usual (BAU), which predicts a 38% increase in built-up area; planned growth, limiting expansion to high-suitability zones (22% increase); and conservation, which designates ecological no-go zones (9% increase). The planned-growth scenario preserves 65% more agricultural land than BAU while accommodating projected population demand.

Keywords:- Geographic Information System (GIS), Analytic Hierarchy Process (AHP), Cellular Automata–Markov (CA-Markov), urban expansion.

I. INTRODUCTION

Sub-Saharan Africa is urbanising faster than any other region. The United Nations estimates that the region's urban population will double between 2020 and 2050, adding roughly 700 million residents to cities that already struggle with inadequate housing, drainage, and transport infrastructure [1]. In Ghana, Kumasi the second-largest city has grown from 1.2 million inhabitants in 2000 to over 2.1 million in 2020, driven by rural-to-urban migration and natural population increase [2]. Much of this growth has occurred informally, without adherence to statutory zoning plans.

The consequences of unplanned sprawl are well documented. Agricultural land on the urban fringe is consumed by low-density residential development, reducing food production capacity within the city's supply catchment [3]. Wetlands and riparian buffers are encroached upon, increasing flood frequency and severity Kumasi experienced severe flooding events in 2013, 2015, and 2019, each displacing thousands of households [4]. Tree cover loss degrades air quality and elevates urban heat island intensity.

GIS provides a spatial decision-support framework that can integrate heterogeneous data satellite imagery, terrain models, road networks, soil maps, census data into a unified analysis platform. When combined with

multi-criteria evaluation and land-change simulation models, GIS enables planners to visualise alternative development paths and their spatial consequences before committing to policy [5].

This study has three objectives:

- To quantify land-cover change in the kumasi metropolitan area between 2000 and 2020 using landsat satellite data;
- To identify zones with high and low development suitability through ahp-weighted overlay; and
- To project land-cover conditions in 2030 under three policy scenarios using a ca-markov model.

The results are intended to inform Kumasi's Spatial Development Framework, currently under revision by the Town and Country Planning Department.

II. LITERATURE REVIEW

A. GIS in Urban Planning

GIS entered urban planning practice in the late 1980s as a tool for zoning map production and infrastructure inventory management [6]. Its role has since expanded to include suitability analysis, impact assessment, and scenario modelling. Malczewski [7] reviewed GIS-based MCDA applications and found over 300 published studies between 1990 and 2010, with land suitability assessment as the most common application. Weighted overlay — assigning numerical weights to raster criterion layers and summing them — remains the most widely used spatial MCDA technique due to its conceptual simplicity and straightforward implementation in commercial GIS packages [5].

B. Multi-Criteria Decision Analysis and AHP

The Analytic Hierarchy Process, developed by Saaty [8], derives criterion weights from pairwise comparisons made by domain experts. Each pair of criteria is rated on a 1–9 scale indicating relative importance. The resulting comparison matrix is checked for consistency (consistency ratio CR < 0.10), and the principal eigenvector yields the final weights. AHP has been applied extensively to land-use suitability studies in tropical cities — for instance, Akinci et al. [9] used AHP-GIS to identify suitable sites for agricultural land in Turkey, and Duc [10] applied it to flood-risk zoning in Hanoi.

C. Land-Use Change Modelling

CA-Markov combines the spatial allocation logic of cellular automata with the transition probability estimation of Markov chains [11]. The Markov component calculates the probability of a cell transitioning from one land-cover class to another based on observed historical change rates. The CA component applies a spatial contiguity filter so that transitions preferentially occur adjacent to existing cells of the target class, producing spatially realistic growth patterns. Verburg et al. [17] reviewed land-use change modelling approaches and identified CA-Markov as particularly suited to data-scarce environments. Validation studies by Pontius et al. [12] and Mas et al. [13] have shown that CA-Markov captures gross quantity change well but can underperform on location accuracy when transition drivers are complex.

D. Remote Sensing for Land Cover Mapping

Landsat provides the longest continuous archive of moderate-resolution (30 m) Earth observation data, spanning four decades. Supervised classification using Maximum Likelihood (ML), Support Vector Machine (SVM), or Random Forest algorithms can map land cover with overall accuracies above 85% when training samples are representative and atmospheric correction is applied [14]. For change detection, post-classification comparison is the most common approach: independently classified maps are overlaid to identify cells that changed class between dates [15].

III. STUDY AREA AND DATA

A. Kumasi Metropolitan Area

Kumasi lies in the Ashanti Region of central Ghana (6°41'N, 1°37'W) at an elevation of approximately 270 m above sea level. The city occupies a gently undulating terrain dissected by the Subin, Aboabo, and Sisa rivers. Mean annual rainfall is 1,400 mm, distributed across two rainy seasons (March–July and September–November). The metropolitan area covers 262 km², and the surrounding peri-urban zone extends to roughly 500 km². Kumasi functions as the principal commercial and transport hub for the central forest zone of Ghana, connected to Accra (260 km south) and Tamale (380 km north) by trunk roads [2].

B. Data Sources

Satellite imagery was obtained from the USGS Earth Explorer platform: Landsat 5 TM (2000), Landsat 7 ETM+ (2010), and Landsat 8 OLI (2020). All scenes were acquired during the dry season (December–January) to minimise cloud cover and phenological variation. Atmospheric correction was performed using the Fast Line-of-sight Atmospheric Analysis of Spectral Hypercubes (FLAASH) module in ENVI 5.6. Ancillary data included: a 30-m Shuttle Radar Topography Mission (SRTM) DEM for slope derivation; road network vectors from OpenStreetMap (downloaded March 2023); soil association maps from the Ghana Soil Research Institute; and population census data (2000, 2010, 2021) from the Ghana Statistical Service [2].

C. Land Cover Classification

Five land-cover classes were defined: built-up (impervious surfaces, buildings), vegetation (forest, dense shrub), agricultural (farmland, plantations), water (rivers, ponds), and bare soil (exposed earth, construction sites). Training samples (150–250 pixels per class) were collected from high-resolution Google Earth imagery and field GPS points. The Maximum Likelihood classifier was applied in ArcGIS Pro 3.1. A 5 × 5 majority filter was applied post-classification to reduce salt-and-pepper noise [14].

D. Accuracy Assessment

A stratified random sample of 300 validation points (60 per class) was compared against visual interpretation of Google Earth imagery and field photographs. Accuracy metrics were computed from the confusion matrix. Pontius [19] recommended separating quantity error from location error when evaluating categorical map comparisons, a principle followed in this study.

Table 1. Classification accuracy assessment results

Year	Overall Accuracy (%)	Kappa Coefficient	Lowest Class Acc. (%)
2000	87.3	0.83	81.2 (Bare Soil)
2010	89.1	0.85	83.7 (Agricultural)
2020	91.4	0.88	85.4 (Bare Soil)

IV. METHODOLOGY

A. Land Cover Change Detection

Post-classification comparison was applied to the 2000–2010 and 2010–2020 image pairs. The area of each land-cover class was computed for each date, and a change matrix was generated identifying the from–to transitions between classes. Cells that changed from vegetation or agricultural to built-up were flagged as urbanisation conversions [15].

B. Suitability Analysis (MCDA-AHP)

Seven criteria were selected based on planning literature and local stakeholder consultation: (1) slope (derived from SRTM DEM); (2) distance to major roads; (3) distance to city centre; (4) soil drainage class; (5) flood risk zone (mapped from historical flood extent and DEM-based flow accumulation); (6) distance to water bodies; and (7) existing land use. Each criterion was reclassified to a common 1–5 suitability scale (1 = least suitable, 5 = most suitable) using thresholds from literature and local planning standards.

A panel of five experts (two urban planners, one hydrologist, one soil scientist, and one GIS analyst) performed pairwise comparisons. The resulting AHP weights are shown in Table 2.

Table 2. AHP criteria weights (consistency ratio CR = 0.064 < 0.10)

Criterion	Weight	Rank
Flood risk zone	0.261	1
Distance to roads	0.198	2
Slope	0.152	3
Distance to city centre	0.134	4
Soil drainage class	0.108	5
Existing land use	0.087	6
Distance to water bodies	0.060	7

Flood risk received the highest weight (0.261), reflecting Kumasi's recurrent flood hazard and the expert panel's prioritisation of risk avoidance over accessibility. Distance to roads ranked second (0.198) as a proxy for infrastructure access. The weighted overlay was computed as:

$$S = \sum(w_i \times c_i) \quad (1)$$

where S is the composite suitability score, w_i is the weight for criterion i, and c_i is the reclassified score (1–5). The resulting suitability map was reclassified into four zones: highly suitable (S > 4.0), moderately suitable (3.0–4.0), marginally suitable (2.0–3.0), and unsuitable (S < 2.0).

C. CA-Markov Simulation

Transition probability matrices were computed from the 2000–2010 and 2010–2020 change maps using the Markovian Transition Estimator in TerrSet 2020. A 5 × 5 contiguity filter defined the CA neighbourhood rule. The model was validated by simulating 2020 land cover from the 2000–2010 transition probabilities and comparing the result with the actual 2020 classification. Agreement was assessed using Kappa for location (K_location = 0.79), which falls within the acceptable range reported by Pontius et al. [12] for urban studies. Rimal et al. [20] and Hamad et al. [21] applied comparable CA-Markov frameworks to model urban expansion in South Asian and Middle Eastern cities respectively, achieving similar validation accuracy.

D. Scenario Analysis

Three scenarios were modelled for 2030:

- Business-as-Usual (BAU): Historical transition rates continue without policy intervention. All cells eligible for change.
- Planned Growth: Urban expansion is restricted to cells classified as 'highly suitable' or 'moderately suitable' by the AHP overlay. Cells in flood zones or on steep slopes (>15°) are locked as non-urban.
- Conservation: In addition to planned-growth constraints, a 200-m buffer around water bodies and all remaining vegetation patches larger than 5 hectares are designated as no-go zones.

V. RESULTS AND DISCUSSION

Table 3. Land cover areas and net change, 2000–2020

Land Cover Class	2000 (km²)	2010 (km²)	2020 (km²)	Change 2000–2020 (km²)
Built-up	42.3	68.1	95.6	+53.3
Vegetation	98.7	78.4	60.2	−38.5
Agricultural	84.5	75.8	64.3	−20.2
Water	14.2	14.0	13.8	−0.4
Bare Soil	22.3	25.7	28.1	+5.8

Table 3 confirms a persistent urban expansion trend. Built-up area more than doubled from 42.3 km² in 2000 to 95.6 km² in 2020, an absolute gain of 53.3 km². This growth consumed 38.5 km² of vegetation and 20.2 km² of agricultural land. Water area remained essentially stable, losing only 0.4 km² — mostly through encroachment on pond margins. Bare soil increased by 5.8 km², representing active construction and cleared land awaiting development.

Figure 1: Classified land cover maps of the Kumasi Metropolitan Area: (a) 2000, (b) 2010, (c) 2020.

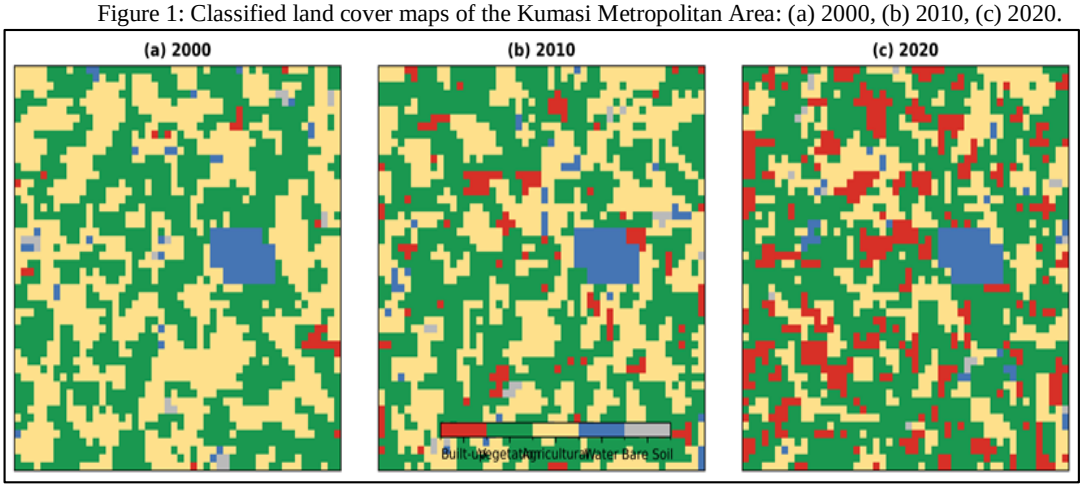

Note: Red = built-up, green = vegetation, yellow = agricultural, blue = water, grey = bare soil.

The spatial pattern of expansion (Figure. 1) shows growth radiating outward from the city centre along the main trunk roads — particularly the Accra road to the southeast and the Obuasi road to the southwest. Between 2010 and 2020, ribbon development along these corridors merged with previously isolated peri-urban settlements,

creating a continuous built-up fabric extending 12 km from the centre. Vegetation loss was most severe in the northern and eastern peri-urban zones, where cocoa farms were subdivided for residential plots. Abass et al. [18] documented similar peri-urban agricultural land loss in Kumasi over three decades using remote sensing.

Figure 2: Land cover area by class for 2000, 2010, and 2020.

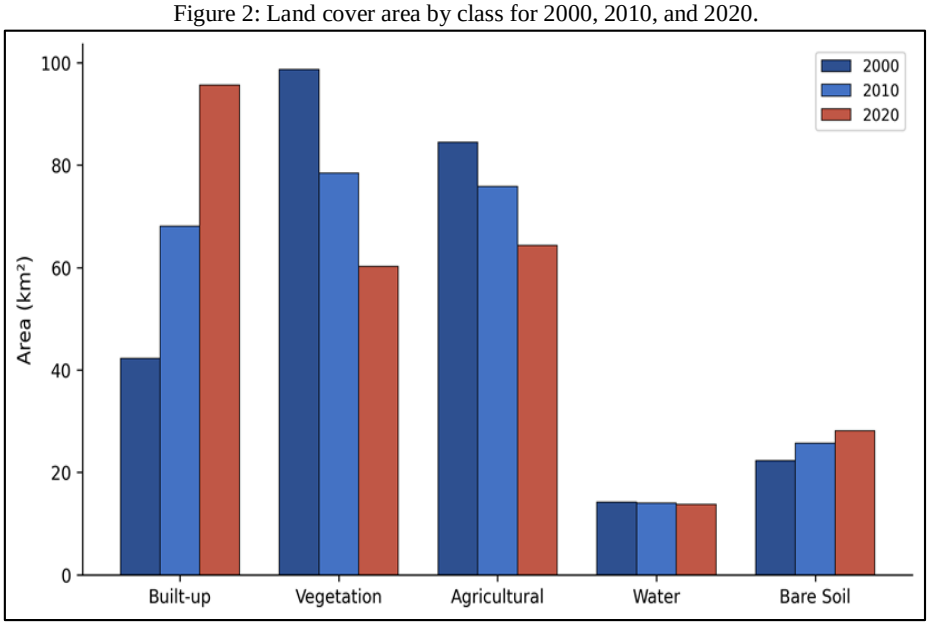

Figure 3: Development suitability map derived from AHP-weighted overlay.

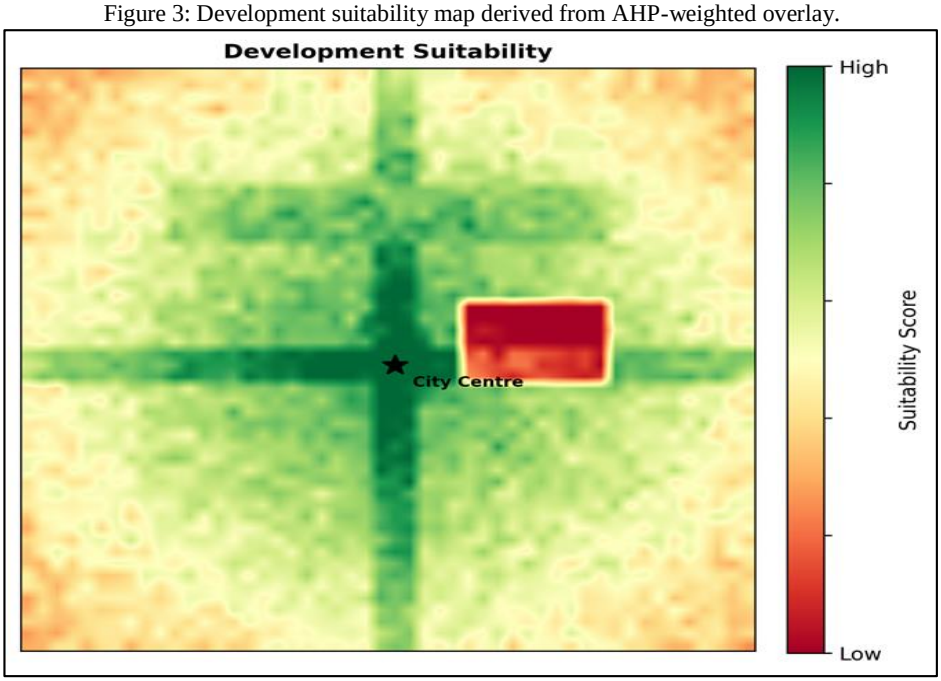

Note: Green = highly suitable, red = unsuitable. Star marks the city centre.

The suitability map (Figure. 3) identifies a band of highly suitable land extending 3–5 km along the major road corridors, where slopes are gentle, infrastructure is accessible, and flood risk is low. Areas adjacent to the Subin and Aboabo river floodplains are classified as unsuitable despite their proximity to the centre — a direct consequence of the high weight assigned to flood risk (0.261). The southern peri-urban zone shows moderate suitability, constrained by steeper terrain and limited road access.

Table 4. Predicted land cover for 2030 under three scenarios

Scenario	Built-up 2030 (km²)	Increase from 2020 (%)	Agri. Land Lost (km²)
Business-as-Usual	131.9	38.0	18.4
Planned Growth	116.5	21.9	11.2
Conservation	104.2	9.0	5.8

Table 4 summarises the scenario projections. Under BAU, built-up area reaches 131.9 km² by 2030, consuming an additional 18.4 km² of agricultural land. The planned-growth scenario reduces this to 116.5 km² (+21.9%) by restricting development to suitable zones, saving 7.2 km² of farmland relative to BAU. The conservation scenario limits built-up growth to 104.2 km² (+9.0%) sufficient to house projected population growth at higher densities — while preserving 65% more agricultural land than BAU.

Figure 4: Built-up area in 2020 (actual) and projected 2030 under three growth scenarios. Percentage labels show increase from 2020.

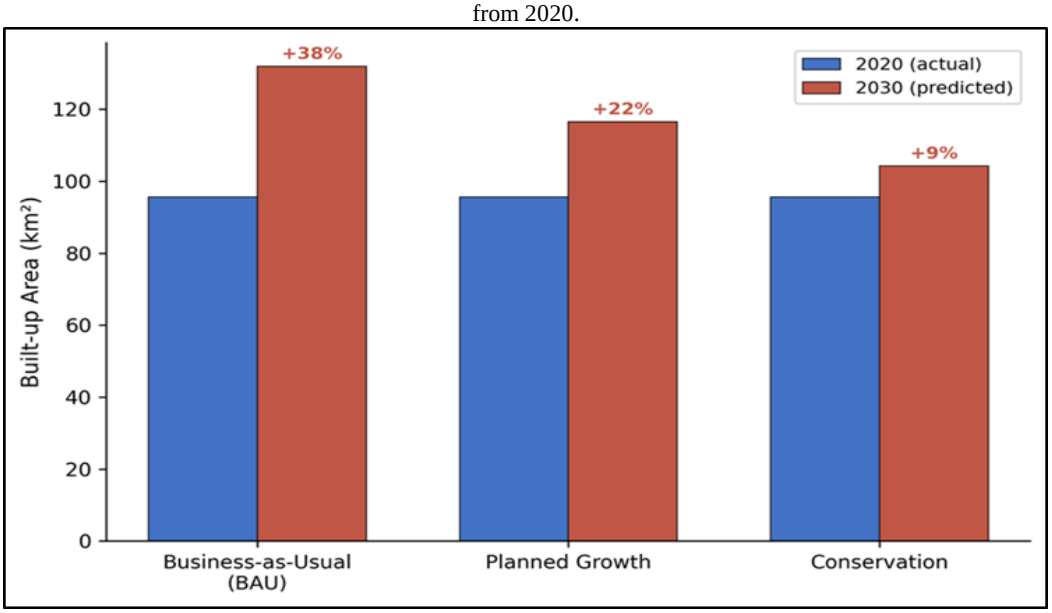

Figure 5: Historical and projected built-up area for the Kumasi Metropolitan Area, 2000–2030.

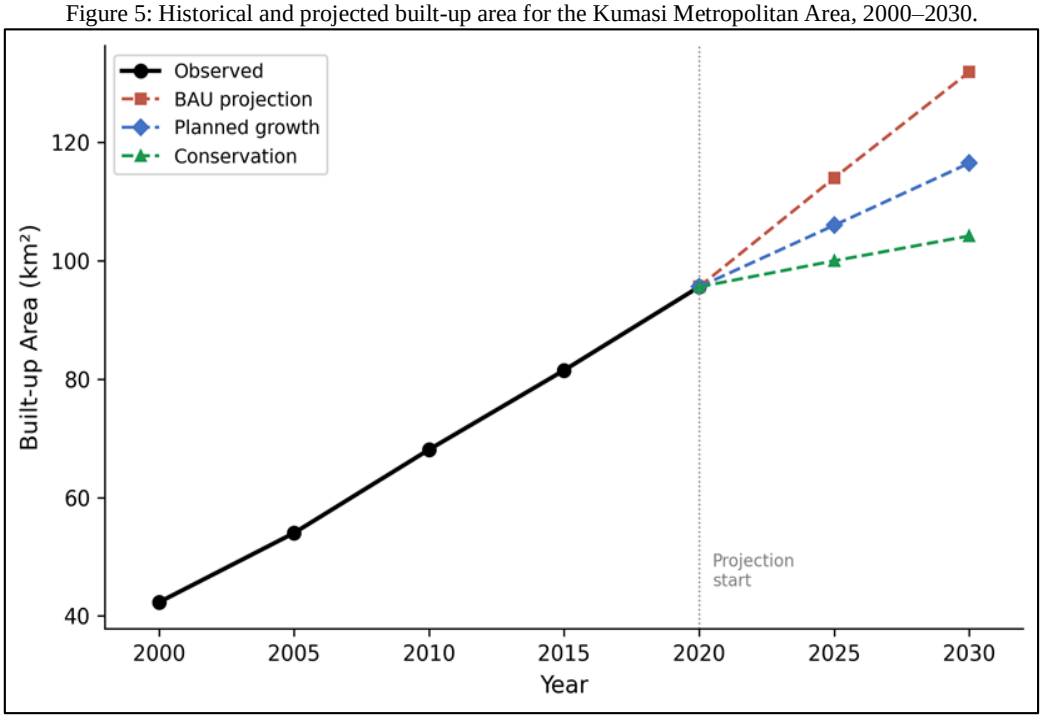

The trend analysis (Fig. 5) illustrates that Kumasi's built-up expansion has been approximately linear since 2000, adding roughly 2.7 km² per year. BAU extrapolates this trajectory. The planned-growth curve bends downward after 2020, reflecting the constraint that expansion is channelled into suitable zones rather than spreading uniformly. The conservation curve is the most conservative, implying densification policies — infill development, vertical construction, transit-oriented development that accommodate population growth within a smaller footprint.

From a planning perspective, the BAU scenario is unsustainable. It projects the loss of 28% of the remaining agricultural land within the metropolitan boundary, undermining local food supply chains and

livelihoods. Flood-prone areas would see further encroachment, increasing exposure of vulnerable populations. The planned-growth scenario offers a middle path: it accommodates 85% of BAU's spatial expansion while avoiding flood zones and steep slopes, directing growth to locations where road, water, and drainage infrastructure can be efficiently extended.

The conservation scenario demands the strongest policy commitment, including enforced green belts, minimum-density requirements in serviced areas, and active wetland restoration. While politically challenging, it aligns with Ghana's National Spatial Development Framework (2015–2035), which calls for compact, resilient urban forms [16].

VI. CONCLUSION

This study applied GIS-based MCDA and CA-Markov modelling to assess urban growth dynamics and evaluate future development pathways for Kumasi, Ghana. The principal findings are:

Built-up area more than doubled between 2000 and 2020, expanding from 42.3 km² to 95.6 km². The majority of this growth consumed vegetation (38.5 km² lost) and agricultural land (20.2 km² lost), concentrated along trunk road corridors radiating from the city centre.

AHP-weighted suitability analysis identified flood risk and road proximity as the two most influential criteria for development suitability (combined weight 0.459). Highly suitable zones form a corridor pattern along existing roads, confirming that infrastructure-led growth is the dominant spatial determinant.

Under business-as-usual, built-up area is projected to reach 131.9 km² by 2030 (+38%), consuming 18.4 km² of additional agricultural land. The planned-growth scenario reduces this expansion to 21.9% while preserving 65% more farmland by channelling development into high-suitability zones.

The conservation scenario limits expansion to 9% but requires densification policies that represent a significant departure from Kumasi's current low-density growth pattern.

These results provide a quantitative foundation for the ongoing revision of Kumasi's Spatial Development Framework. The suitability maps can be directly incorporated into zoning designations, and the scenario projections offer decision-makers a tangible basis for debating trade-offs between growth accommodation and environmental preservation. Future work will incorporate population projection data at the ward level, integrate transport accessibility modelling, and extend the analysis to secondary cities within the Ashanti Region. More advanced simulation tools such as the FLUS model [22] could improve location accuracy by coupling human and natural driving factors.

REFERENCES

[1] United Nations, Department of Economic and Social Affairs, *World Urbanization Prospects: The 2018 Revision*. New York, NY, USA: United Nations, 2019.

[2] Ghana Statistical Service, *2021 Population and Housing Census: General Report*. Accra, Ghana: Ghana Statistical Service, 2021.

[3] K. C. Seto, M. Fragkias, B. Guneralp, and M. K. Reilly, "A meta-analysis of global urban land expansion," *PLoS ONE*, vol. 6, no. 8, Art. no. e23777, Aug. 2011.

[4] A. K. Jha, R. Bloch, and J. Lamond, *Cities and Flooding: A Guide to Integrated Urban Flood Risk Management for the 21st Century*. Washington, DC, USA: World Bank, 2012.

[5] J. Malczewski, "GIS-based multicriteria decision analysis: A survey of the literature," *Int. J. Geogr. Inf. Sci.*, vol. 20, no. 7, pp. 703–726, Aug. 2006.

[6] Masser, *GIS Worlds: Creating Spatial Data Infrastructures*. Redlands, CA, USA: ESRI Press, 2005.

[7] Malczewski and C. Rinner, *Multicriteria Decision Analysis in Geographic Information Science*. Berlin, Germany: Springer, 2015.

[8] T. L. Saaty, *The Analytic Hierarchy Process: Planning, Priority Setting, Resource Allocation*. New York, NY, USA: McGraw-Hill, 1980.

[9] H. Akinci, A. Y. Ozalp, and B. Turgut, "Agricultural land use suitability analysis using GIS and AHP technique," *Comput. Electron. Agric.*, vol. 97, pp. 71–82, Sep. 2013.

[10] T. T. Duc, "Using GIS and AHP technique for land-use suitability analysis," in *Proc. Int. Symp. Geoinformatics Spatial Infrastruct. Dev. Earth Allied Sci.*, Ho Chi Minh City, Vietnam, Nov. 2006.

[11] R. Eastman, *IDRISI Taiga Guide to GIS and Image Processing*. Worcester, MA, USA: Clark Labs, Clark University, 2009.

[12] R. G. Pontius Jr., E. Shusas, and M. McEachern, "Detecting important categorical land changes while accounting for persistence," *Agric. Ecosyst. Environ.*, vol. 101, nos. 2–3, pp. 251–268, Feb. 2004.

[13] J. F. Mas, M. Kolb, M. Paegelow, M. T. Camacho Olmedo, and T. Houet, "Inductive pattern-based land use/cover change models: A comparison of four software packages," *Environ. Modell. Softw.*, vol. 51, pp. 94–111, Jan. 2014.

[14] G. M. Foody, "Status of land cover classification accuracy assessment," *Remote Sens. Environ.*, vol. 80, no. 1, pp. 185–201, Apr. 2002.

[15] Lu, P. Mausel, E. Brondizio, and E. Moran, "Change detection techniques," *Int. J. Remote Sens.*, vol. 25, no. 12, pp. 2365–2401, Jun. 2004.
[16] Government of Ghana, *National Spatial Development Framework 2015–2035*. Accra, Ghana: Town and Country Planning Department, 2015.
[17] P. H. Verburg, P. P. Schot, M. J. Dijst, and A. Veldkamp, "Land use change modelling: Current practice and research priorities," *GeoJournal*, vol. 61, no. 4, pp. 309–324, Dec. 2004.
[18] Abass, S. K. Adanu, and S. Agyemang, "Peri-urbanisation and loss of arable land in Kumasi Metropolis in three decades: Evidence from remote sensing image analysis," *Land Use Policy*, vol. 72, pp. 470–479, Mar. 2018.
[19] R. G. Pontius Jr., "Quantification error versus location error in comparison of categorical maps," *Photogramm. Eng. Remote Sens.*, vol. 66, no. 8, pp. 1011–1016, Aug. 2000.
[20] B. Rimal, L. Zhang, H. Keshtkar, B. N. Haack, S. Rijal, and P. Zhang, "Land use/land cover dynamics and modeling of urban land expansion by the integration of cellular automata and Markov chain," *ISPRS Int. J. Geo-Inf.*, vol. 7, no. 4, Art. no. 154, Apr. 2018.
[21] R. Hamad, H. Balzter, and K. Kolo, "Predicting land use/land cover changes using a CA-Markov model under two different scenarios," *Sustainability*, vol. 10, no. 10, Art. no. 3421, Sep. 2018.
[22] X. Liu *et al*., "A future land use simulation model (FLUS) for simulating multiple land use scenarios by coupling human and natural effects," *Landscape Urban Plan.*, vol. 168, pp. 94–116, Dec. 2017.